

Design of SiC Capacitive Pressure Sensor with LC-Based Oscillator Readout Circuit

Azza M. Anis, M. M. Abutaleb, Hani F. Ragai, and M. I. Eladawy

Abstract—This paper presents the characterization and design of a capacitive pressure sensor with LC-based 0.35 μm CMOS readout circuit. SPICE is employed to evaluate the characteristics of the readout circuit and COMSOL multiphysics structural analysis is used to simulate the behavior of the pressure sensor. The readout circuit converts the capacitance variation of the pressure sensor into the frequency output. Simulation results show that the proposed pressure sensor has output frequency from 2.50 to 2.28 GHz in a pressure range from 0.1 to 2 MPa almost linearly. The sensitivity of the frequency shift with respect to the applied pressure load is 0.11 GHz/MPa.

Keywords—CMOS LC-based oscillator, micro pressure sensor, silicon carbide

I. INTRODUCTION

SMART micro pressure sensors are of increasing demand in a wide range of applications, including those in distributed sensing and control systems, automotive industry, instrumentation, industrial process automation, nuclear and power station, and environmental monitoring [1]–[4]. Hence, there is a growing need for a generic interface for use with pressure sensors in smart portable and wireless microsystems applications. Such circuits should be able to read out a wide range of capacitance and sensitivity of pressure sensors, dissipate low power, and occupy very small area with no external components. There have been numerous readout circuits introduced for micro sensors. The operational amplifier is used to convert the current variation of the pressure sensor into the voltage output [5]. A stable multivibrator circuit is used as a readout circuitry for the pressure microsensor [6]. The capacitance-to-pulse-width converter circuit is demonstrated for the operation in ubiquitous sensor network [7].

Azza M. Anis is with the Electronics, Communication, and Computer Department, Helwan University, Cairo, Egypt (e-mail: azzam.anis@yahoo.com).

M. M. Abutaleb is with the Electronics, Communication, and Computer Department, Helwan University, Cairo, Egypt (e-mail: mostafaengineer@hotmail.com).

Hani F. Ragai is with the Electronics, Communication, and Computer Department, Ain Shams University, Cairo, Egypt (e-mail: hfragai@gmail.com).

M. I. Eladawy is with the Electronics, Communication, and Computer Department, Helwan University, Cairo, Egypt (e-mail: mohamed@eladawy.com).

In this paper, a cross-coupled CMOS LC oscillator based on a capacitance to frequency conversion operation is demonstrated for capacitive pressure sensor applications. The cross-coupled CMOS LC oscillator topology was chosen because it has very few transistors, is easy to implement, and is differential in nature, thus making it easier to generate oscillation signals. Moreover, this topology consumes lower power, which is very suitable for wireless telecommunication applications. Another advantage of this architecture is the easy computation of the LC tank that determines the fundamental frequency of the oscillator.

The paper is structured as follows. The architecture of the cross-coupled CMOS LC oscillator topology is illustrated in Section II. In Section III, the materials of sensor diaphragm will be debated. The simulated results are presented in Section IV. Finally, Section V contains the conclusions.

II. ARCHITECTURE OF THE INTERFACE CIRCUIT

A. Structure of CMOS LC Oscillator

The cross-coupled CMOS LC oscillator is used as a capacitance to frequency conversion circuit. The CMOS oscillator is directly read the capacitance changes due to the applied pressure and converts it into the frequency output. Fig. 1 (a) shows a schematic diagram of the oscillator circuit, which consists of NMOS and PMOS cross-coupled pairs in parallel with LC tank [8]. To achieve steady-state oscillation, the parasitic resistance of the LC tank must be canceled with the negative resistance produced by NMOS and PMOS cross-coupled pairs. When this condition is satisfied, the circuit becomes lossless and generates oscillation. The inductor of the LC tank is implemented by the spiral inductor. The capacitance of the pressure sensor is equivalent to the capacitance of the tank. The output frequency of CMOS oscillator is given by:

$$f = \frac{1}{2\pi} \sqrt{\frac{1}{LC}} \quad (1)$$

Where C presents the sum of all capacitance at the output node. In fig. 1 (b) the total negative resistance of the CMOS cross-coupled pairs can be expressed as a parallel combination of the NMOS and PMOS pair's negative resistance R_{inn} and R_{inp} as:

$$R_{negative} = R_{inn} // R_{inp} = \frac{2}{G_{nn} + G_{mp}} \quad (2)$$

The negative transconductance of the CMOS cross-coupled pairs is given by the relation:

$$G_m = \left(\frac{G_{mn} + G_{mp}}{2} \right) \quad (3)$$

If all losses in the LC tank are equal to the equivalent parallel resistance R_p . So the tank transconductance is $G_{\text{tank}} = 1/R_p$. Then for the oscillation to start and to compensate for tank losses, the negative transconductance associated with the active devices (NMOS and PMOS transistor pairs) should be greater than the tank transconductance $G_m = \alpha G_{\text{tank}}$, and α is a start-up safety factor ($\alpha = 3.5$ as in [9]).

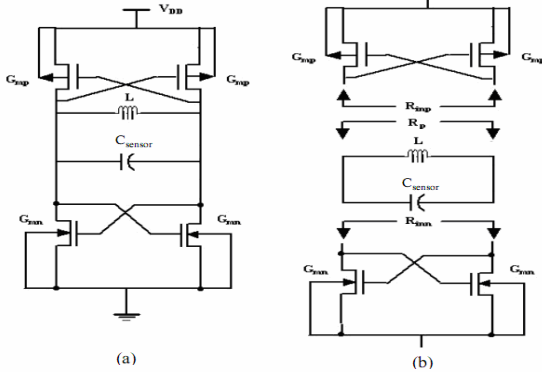


Fig. 1 (a) Schematic diagram of CMOS cross-coupled oscillator circuit and (b) Calculation of total negative resistance of CMOS oscillator

B. Structure of the Capacitive Pressure Sensor

The fundamental structure of the capacitive pressure sensor can be regarded to be a series of parallel plate capacitors consisting of the top electrode of sensitive diaphragms and the bottom electrode formed on the stationary substrate. The applied pressure load causes the diaphragm to deflect and the capacitance to change. Sensor diaphragms can be described by plate theory [10]. In plate theory, the deflection Y of a clamped circular plate under a uniform applied pressure load P is described by:

$$Y(r) = Y_o \left(1 - \left(\frac{r}{a} \right)^2 \right)^2 \quad (4)$$

Where a , r , are the diaphragm radius and the distance of the applied load from the center respectively. Y_o is the maximum deflection and is defined by:

$$Y_o = \frac{Pa^4}{64D} \quad (5)$$

$$D = \frac{Eh^3}{12(1-\nu^2)} \quad (6)$$

Where D , E , h , and ν are bending rigidity, modulus of elasticity, plate thickness, and Poisson ratio respectively.

A sensing cell can be taken as a series of three capacitors and the total capacitance C_t is given by:

$$C_t = \frac{1}{\frac{1}{C_{ox}} + \frac{1}{C_{gap}} + \frac{1}{C_{ox}}} \quad (7)$$

$$C_{gap} = \int_0^{2\pi} \int_0^a \epsilon_o \epsilon_r \frac{r dr d\theta}{g - Y(r)} \quad (8)$$

$$C_{ox} = \epsilon_{ox} \frac{A}{d_{ox}} \quad (9)$$

Where C_{gap} and C_{ox} represent the individual capacitance of the air gap and silicon oxide respectively. ϵ_o is the permittivity of free space, ϵ_r is the permittivity of the air, ϵ_{ox} is the dielectric permittivity of the oxide, g is the air gap at rest, A is the area of diaphragm, d_{ox} is the thickness of silicon oxide. The capacitance of air gap can be evaluated as:

$$C_{gap} = \begin{cases} \frac{\epsilon_o \epsilon_r \pi a^2}{g} & P = 0 \\ 4\epsilon_o \epsilon_r \pi \sqrt{\frac{D}{gP}} \ln \left(\frac{\sqrt{g+a^2} \sqrt{\frac{P}{64D}}}{\sqrt{g-a^2} \sqrt{\frac{P}{64D}}} \right) & P > 0 \end{cases} \quad (10)$$

Assume a capacitive pressure sensor is constructed by 16 sensing cells, so the capacitance C_{sensor} of the pressure sensor can be expressed as:

$$C_{\text{sensor}} = 16.C_t \quad (11)$$

III. MATERIALS FOR DIAPHRAGM

The quality and reproducibility of the materials play a critical role in the commercial viability of the pressure microsensors. Several materials have been used for diaphragm of microsensor such as Aluminum (Al) [11], Stainless Steel [6], Si [12], and compared with Silicon Carbide (SiC) [13]. The displacement at the center of the circular diaphragm and the capacitance between diaphragm and the fixed plate are summarized in table I.

TABLE I
SIMULATION RESULTS FOR DIFFERENT DIAPHRAGM MATERIALS IN THE PRESSURE RANGE UP TO 500 KPA

Symbol	Al	Si	Stainless Steel	SiC
Maximum displacement (μm)	0.45	0.26	0.24	0.12
Capacitance range (pF)	0.97–1.18	0.97–1.07	0.97–1.06	0.97–1.01

It can be seen that the higher young's modulus of SiC, reducing the deflection of device layers experiencing high load forces.

IV. RESULTS

The specifications of the spiral inductor shown in fig. 2 are as follows: $d_{out}=190\text{ }\mu\text{m}$, $s=3\text{ }\mu\text{m}$, $w=10\text{ }\mu\text{m}$, $n=3.5$, $L=2.9\text{ nH}$.

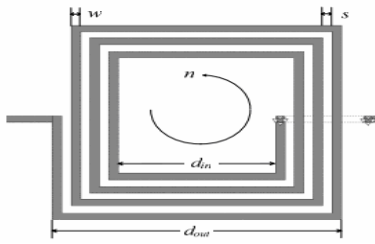


Fig. 2 Schematic of the on chip square spiral inductor [14]

For linear operation of the pressure sensor, Substituting $P=2\text{ MPa}$, $a = 50\text{ }\mu\text{m}$, $h = 2.6\text{ }\mu\text{m}$, $E = 259.5\text{ GPa}$, $\nu = 0.255$, $d_{ox} = 1\text{ }\mu\text{m}$, $g = 0.64\text{ }\mu\text{m}$, $\epsilon_o = 8.85 \times 10^{-12}\text{ F/m}$ and $\epsilon_{ox} = 3.54 \times 10^{-11}\text{ F/m}$, $\epsilon_r = 1$ and $r=0$, we obtain the displacement at the center of the circular plate is about $0.48\text{ }\mu\text{m}$ as shown in fig. 3.

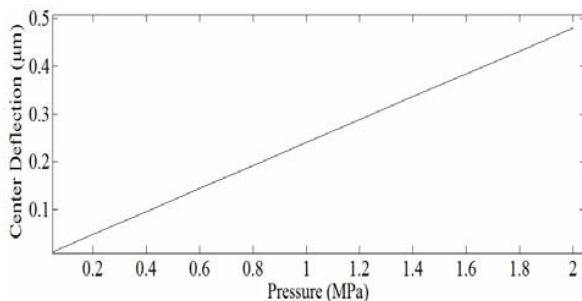


Fig. 3 Center deflection of sensor diaphragm at various pressure loads up to 2 MPa

COMSOL Multiphysics structural analysis has been used to model the circular diaphragm of the sensor. Fig. 4 presents 3D finite element analysis of a sensor diaphragm up to 2 MPa, the maximum center deflection was $0.481\text{ }\mu\text{m}$, which agree with the analytical result obtained from previous Equations.

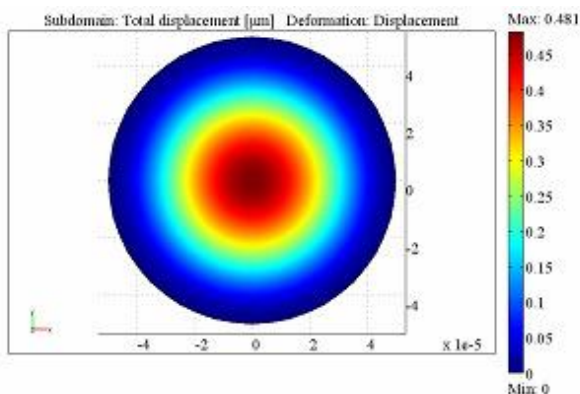


Fig. 4 A 3D finite element simulation of sensor diaphragm using COMSOL

The capacitance of the pressure sensor C_{sensor} changes from 0.97 to 1.21 pF when pressure increased up to 2 MPa as shown in fig. 5.

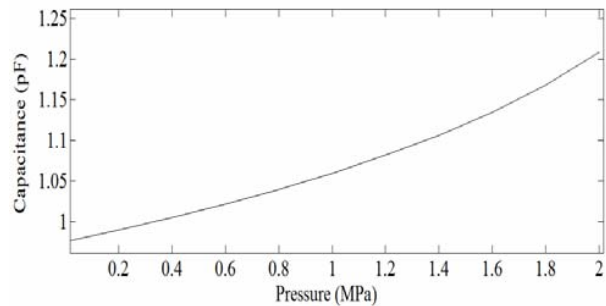


Fig. 5 Capacitance versus different pressure loads

The circuit shown in fig. 1(a) has been simulated by SPICE when $V_{DD} = 2\text{ V}$. The frequency response of the output voltage for the pressure sensor is shown in fig. 6. The results showed that the pressure sensor had an output frequency of 2.50 GHz at 0.1 MPa pressure loads. When increasing the pressure, the output frequency produced a change. The output frequency changed to 2.28 GHz at 2 MPa pressure loads.

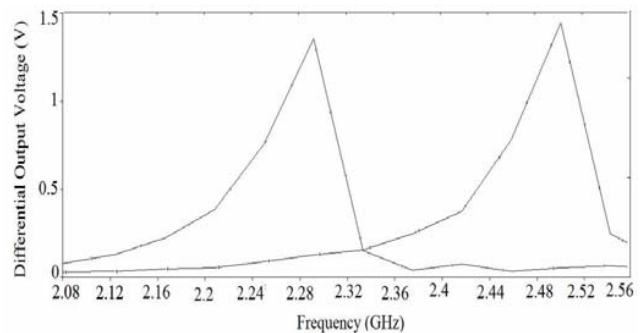


Fig. 6 Frequency response of the pressure sensor

Fig. 7 shows the variation in the capacitance of pressure sensor with the output frequency. Fig. 8 shows the output frequency of LC oscillator as a function of applied pressure loads up to 2 MPa .

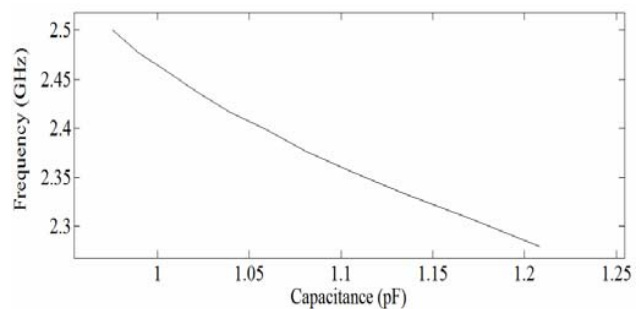


Fig. 7 Capacitance versus output frequency

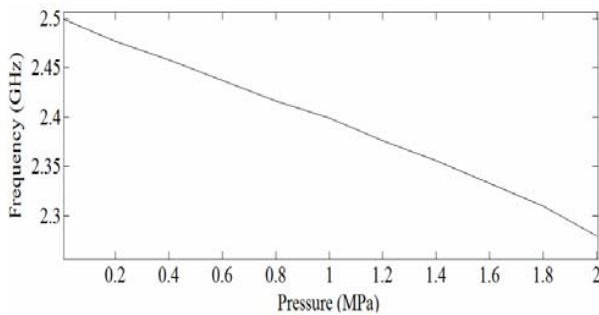


Fig. 8 Simulated results of output frequency in the pressure sensor

The simulated results show that the total frequency shift is 220 MHz with a corresponding capacitance change from 0.97 to 1.21 pF in the pressure range up to 2MPa.

V.CONCLUSION

We present a SiC capacitive pressure micro sensor with a cross-coupled CMOS LC oscillator as an interface circuit for high frequency applications. SiC material was used as a material of sensor's diaphragm for harsh environment sensing applications. The finite element analysis based on COMSOL has been presented to evaluate the deflection of sensor's diaphragm at different pressure loads. The characteristics of the readout circuit were evaluated using SPICE software. The simulated results depicted that, at a low supply voltage of 2 V the capacitive pressure sensor had output frequency range from 2.50 to 2.28 GHz in the pressure range from 0.1 to 2 MPa. The sensitivity of the frequency shift with respect to the applied pressure load is 0.11 GHz/MPa.

REFERENCES

- [1] Eggers T., Marschner C., Marschner U., Clasbrummel B., Laur R., Binder J., "Advanced hybrid integrated low-power telemetric pressure monitoring system for biomedical application," *Proc. IEEE Micro Electro Mech. Syst.*, pp. 329-334, 2000.
- [2] Pulliam W., Russler P., Mlcak R., Murphy K., Kozikowski C., "Micromachined SiC fiber optic pressure sensors for high-temperature aerospace applications," *Proc. SPIE*, pp. 21-30, 2000.
- [3] Huang J.T., Cheng S.C., "Study of injection molding pressure sensor with low cost and small probe," *Sens. Actuators*, pp. 269-274, 2002.
- [4] Berns A., Buder U., Obermeier E., Wolter A., "AeroMEMS sensor array for high-resolution wall pressure measurements," *Sens. Actuators*, pp. 104-111, 2006.
- [5] Dai C.L., Tai Y.W., Kao P.H., "Modeling and fabrication of micro FET pressure sensor with circuits," *Sensors* 7, no. 7, pp. 3386-3398, 2007.
- [6] Sung Pil Chang, Allen, M. G., "Capacitive Pressure Sensors with Stainless Steel Diaphragm and Substrate," *Journal of Micromechanics and Microengineering*, vol. 14, no. 4, pp. 612-618, Apr. 2004.
- [7] Sungsik Lee, Ahra Lee, Chang-Han Je, Myung-Lae Lee, Gunn Hwang, and Chang-Auck Choi, "1.5 V Sub-mW CMOS Interface Circuit for Capacitive Sensor Applications in Ubiquitous Sensor Networks," *ETRI Journal*, vol. 30, no. 5, pp. 644-652, October 2008.
- [8] A. Lacaita, S. Levantino, C. Samori, *Integrated frequency synthesizers for wireless systems*, Cambridge University Press, New York, 2007, ch.4.
- [9] Thomas H. Lee, *The design of CMOS radio-frequency integrated circuits*, 2nd edition, Cambridge University Press, New York, 2004.
- [10] Timoshenko S., Woinosky-Krieger S., "Theory of Plates and Shells," McGraw-Hill Classic Textbook Reissue, 1987, ch. 13.
- [11] Dai C.-L., Lu P.-W., Chang C., Liu C.-Y., "Capacitive Micro Pressure Sensor Integrated with a Ring Oscillator Circuit on Chip," *Sensors* 9, no. 12, pp. 10158-10170, 2009.
- [12] M. Suster, W. H. Ko, D. J. Young, "An Optically Powered Wireless Telemetry Module for High-Temperature MEMS Sensing and Communication," *IEEE Journal of Microelectromechanical Systems*, pp. 536-541, June 2004.
- [13] A. M. Anis, M. M. Abutaleb, H. F. Ragai, M. I. Eladawy, "SiC Capacitive pressure Sensor Node for Harsh Industrial Environment," *CIMSIM*, pp. 413 - 416, Sept. 2011.
- [14] M. Rahimi, S.S. Jamuar, M. N. Hamidon, M. R. Ahmad, S. A. Mousavi, M. Bayat, "Design and Simulation of a 2.4 GHz VCO with High Q MEMS Inductor and CMOS Varactor," *International Journal of Computer and Electrical Engineering*, vol. 1, no. 3, pp. 1793-8163, August 2009.